Supplementary Materials and Methods

RGC axon regeneration

Axon regeneration was examined 14 days after ONC surgery. Optic nerve were dissected, fixed, embedded in OCT medium, and cut into 14μm-thick longitudinal sections on a cryostat as described (1). GAP-43 immunostaining was performed to visualize axon regeneration. GAP-43 positive axons were counted in eight longitudinal sections per eye at 0.5mm and 1mm distance from the injury site.

References:

1. Kurimoto T et al. Long-distance axon regeneration in the mature optic nerve: contributions of oncomodulin, cAMP, and pten gene deletion. *J. Neurosci.* 2010;30(46):15654–63.

2. Busskamp V et al. Genetic reactivation of cone photoreceptors restores visual responses in retinitis pigmentosa. *Science* 2010;329(5990):413–7.

3. Khani SC et al. AAV-Mediated Expression Targeting of Rod and Cone Photoreceptors with a Human Rhodopsin Kinase Promoter. *Invest. Ophthalmol. Vis. Sci.* 2007;48(9):3954–3961.

4. Boshart M et al. A very strong enhancer is located upstream of an immediate early gene of human cytomegalovirus. *Cell* 1985;41(2):521–30.

5. Niwa H, Yamamura K, Miyazaki J. Efficient selection for high-expression transfectants with a novel eukaryotic vector. *Gene* 1991;108(2):193–9.

Figure S1

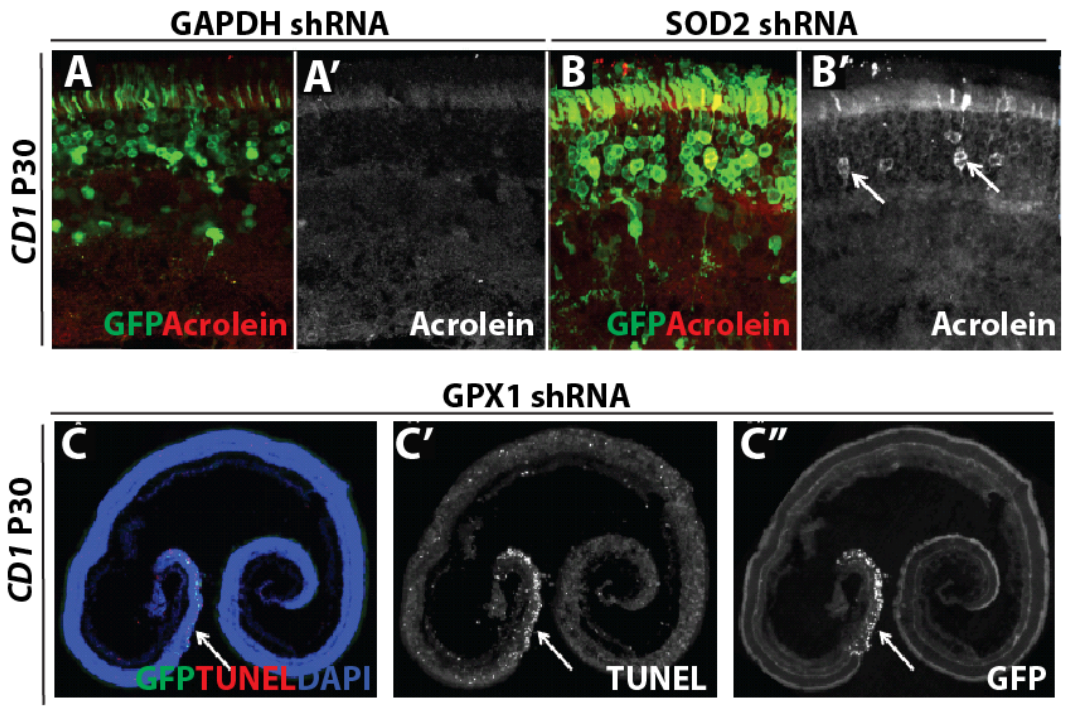

Figure S1. A-B) Knock-down of SOD2 generates oxidation products. A-A') Cross-section from retina at P30 electroporated with control shRNA, stained with anti-GFP (green), and anti-acrolein (red). B-B') SOD2 shRNA, stained with anti-GFP and anti-acrolein, (B') All acrolein positive cells were GFP+. Two examples of acrolein+ cells are indicated by arrows. Upper bracket denotes OS and IS, lower bracket the outer nuclear layer (cell bodies of rods and cones). C) Knock-down of Gpx1 leads to rapid cell death. A low magnification cryosection from retina at P30 stained with DAPI, with electroporated region indicated by the arrow. TUNEL staining (C') revealed positive cells in the area of electroporation, and anti-GFP (C'') shows area that was electroporated is the area with TUNEL+ cells.

Figure S2

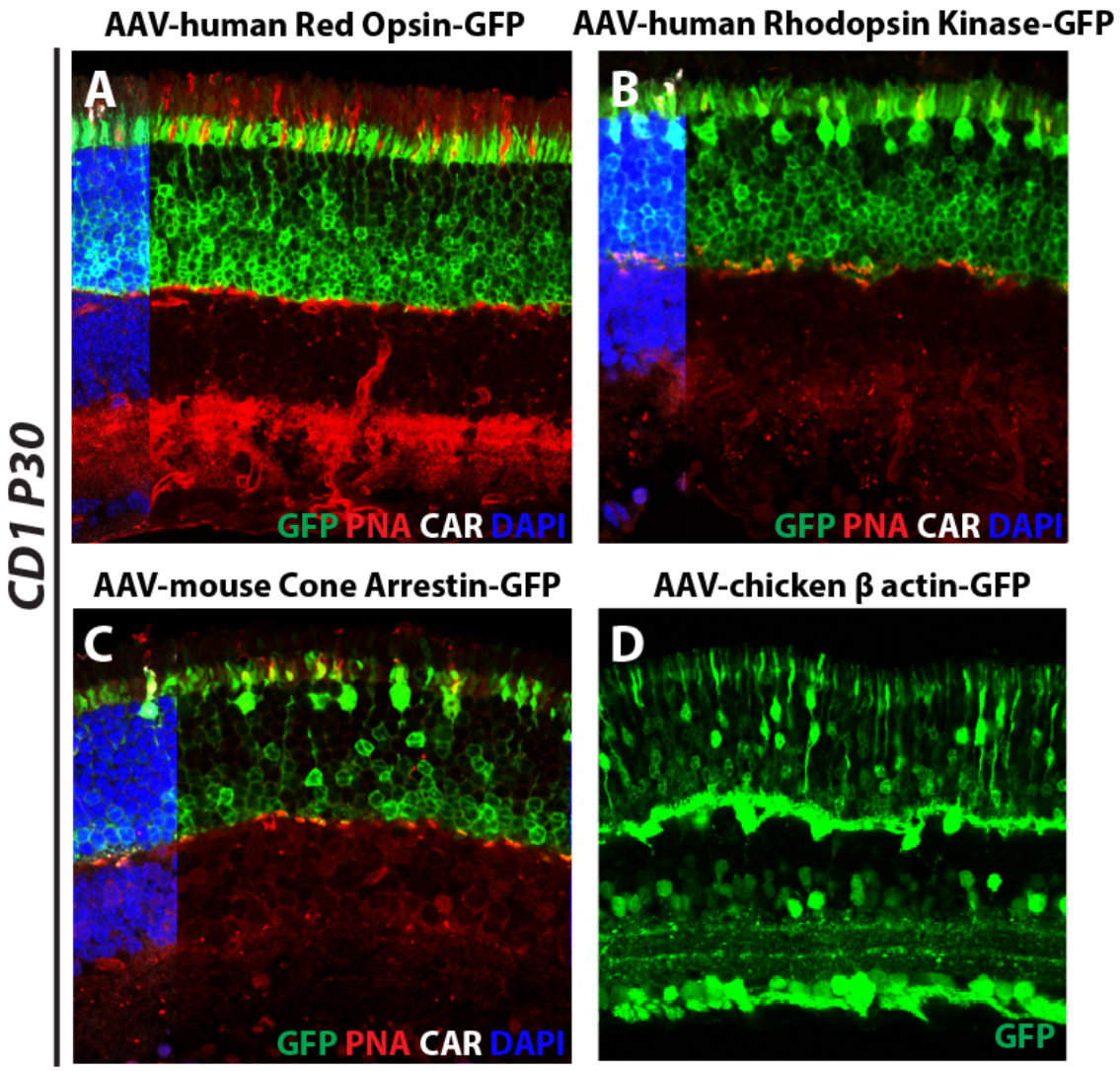

Figure S2. GFP reporter expression driven by different promoters in AAV vectors. All AAV vectors were injected into the subretinal space of neonatal P0 mouse eyes, and retinas were harvested 30 days post infection. Cyrosections of the retinas were stained for the cone marker, cone arrestin (CAR, white), and PNA (red). Green is GFP fluorescence without staining. Human Red Opsin (hRO) promoter (2) (A), human Rhodopsin kinase (hRK) promoter (3) (B), and Mouse Cone Arrestin (mCAR) promoter (2)(C) drives GFP expression in both rods and cones. D) Chicken beta actin (CAG) promoter (4, 5) drives GFP expression in some photoreceptors, horizontal cells, amacrine cells, and ganglion cells.

Figure S3

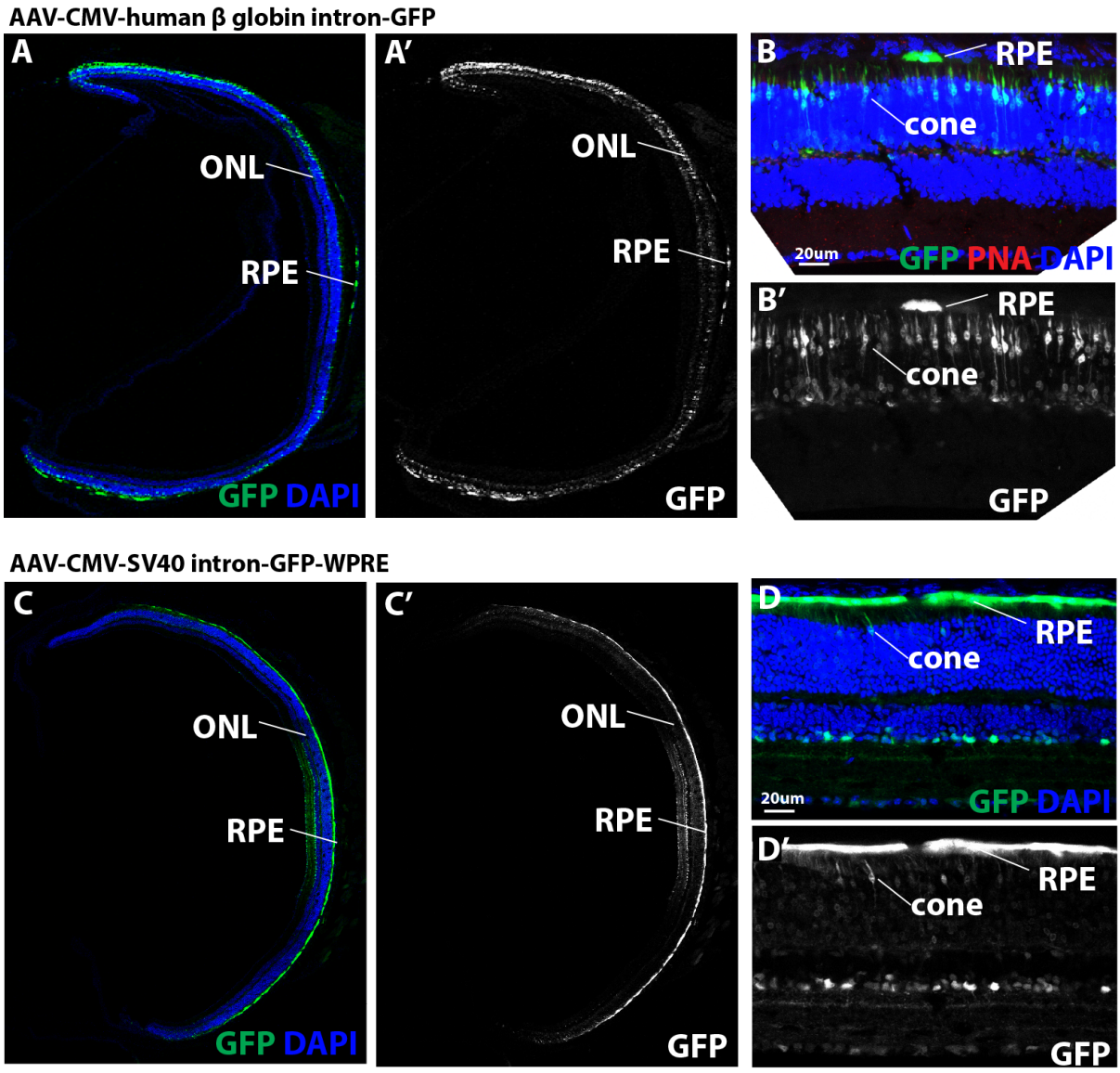

Figure S3. Transduction of RPE cells by AAV-CMV-GFP vectors. A-A') Cross-section of a wild type retina infected by AAV-CMV-GFP vector, which contains a human CMV enhancer/promoter, human β-globin intron, GFP cDNA (construct obtained from Harvard DF/HCC DNA Resource Core). The RPE layer was retained and examined for GFP expression. Few RPE cells expressed GFP. An example of a GFP+ cell is shown in B-B'). C-D) Cross-sections of a wild type retina infected by AAV-CMV-GFP (construct obtained from the University of Pennsylvania virus core facility), which was kindly provided by the gene transfer vector core of Schepens Eye Research Institute, Boston, MA. This vector contains a human CMV enhancer/promoter, SV40 intron, GFP cDNA, woodchuck hepatitis virus posttranscriptional regulatory element (WPRE), and bovine growth hormone polyA (bGH pA), and resulted in high expression in RPE cells. The difference in expression in the RPE between the two vectors may due to the different intron sequence, as both vectors have the same CMV promoter/enhancer sequence and were packaged with the wild type serotype 8 capsids.

Figure S4

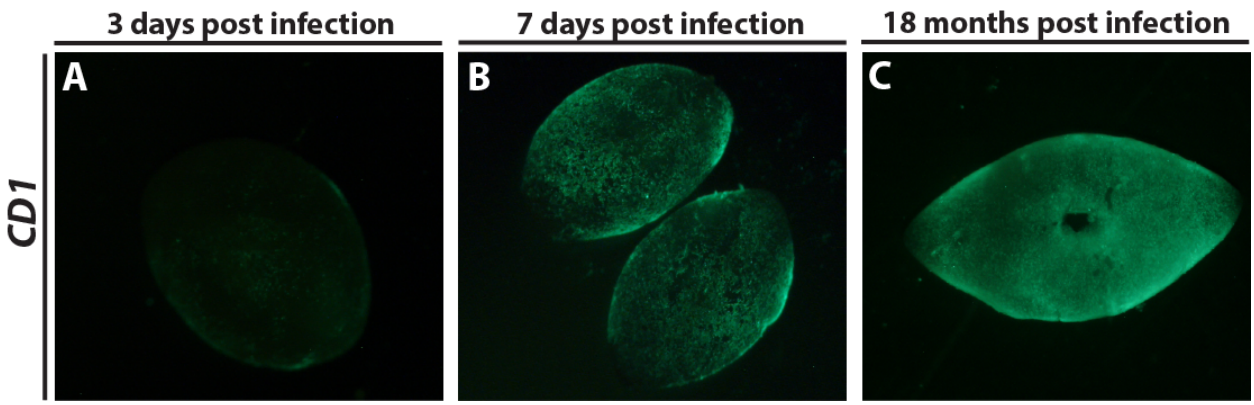

Figure S4. Long-term GFP expression in retina. AAV-GFP vectors were injected subretinally into P0 mouse eyes, and retinas were dissected at 3 days post infection (A), 7 days post infection (B), and 18 months post infection (C) and imaged for native GFP (green).

Figure S5

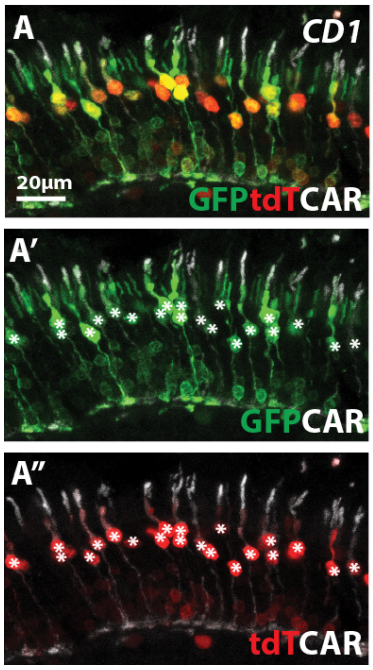

B

AAV-GFP

infectious rate in cones (mean ± s.d.)	titer of vector
99% ± 1% (n=3)	10^{13} gc/ml
99% ± 1% (n=6)	10^{12} gc/ml
15% ± 4% (n=4)	10^{11} gc/ml

AAV-GFP+AAV-tdTomato

coinfectious rate in cones (mean ± s.d.)	titer of vectors
90% ± 5% (n=3)	$2x10^{12}$ gc/ml
50% ± 7% (n=4)	10^{12} gc/ml

Figure S5. A-A'') Cross-section of a wild type retina that was infected by AAV-GFP and AAV-nlstdTomato. GFP (green) and tdTomato (red) were coexpressed in cones, which were marked by staining using anti-cone arrestin (CAR, white, asterisks). B) Quantification of the infection rate of AAV-GFP and the coinfection rate of AAV-GFP and AAV-tdTomato in cones. Numbers shown are mean±s.e.m.; n, number of retinas quantified.

Figure S6

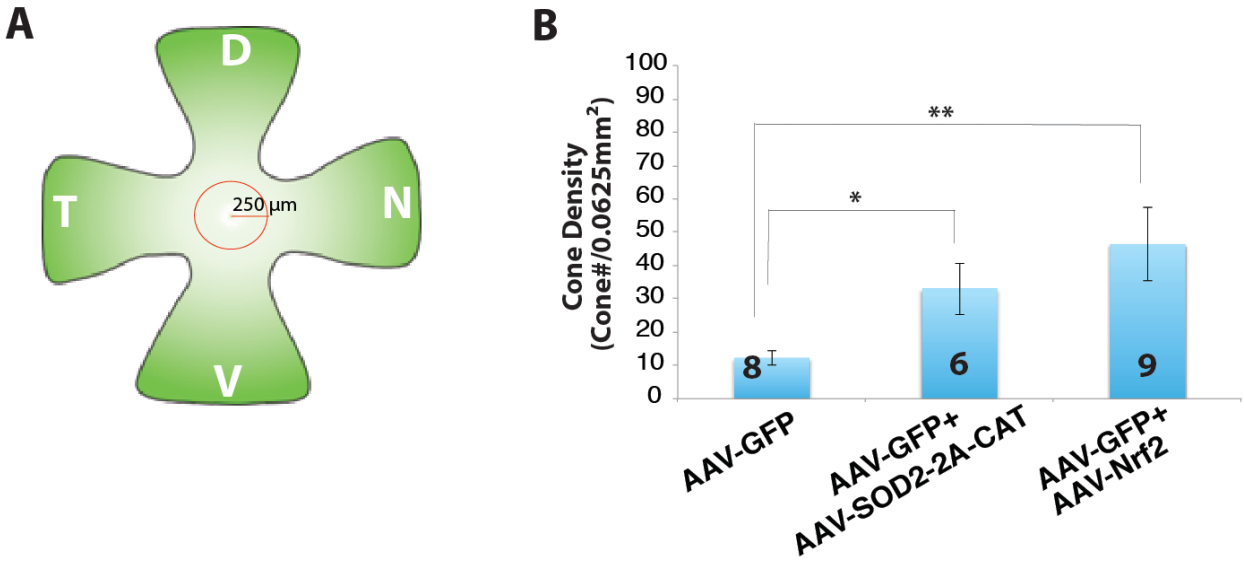

Figure S6. Cone quantification in the central retina. A) Illustration of the quantification scheme. One radius=250 µm circle was placed in the center of a retina. GFP+ cones were counted within the circle, and the cone density was represented as cone#/0.0625 mm^2. B) The cone density of P50 *rd1* retinas infected with AAV-GFP, AAV-GFP+AAV-SOD2-2A-CAT, or AAV-GFP+AAV-Nrf2. The number of retinas quantified for each group is shown at the bottom of each bar. Bars represent mean±s.e.m.. One-way ANOVA test. *$p<0.05$, ** $p<0.01$

Figure S7

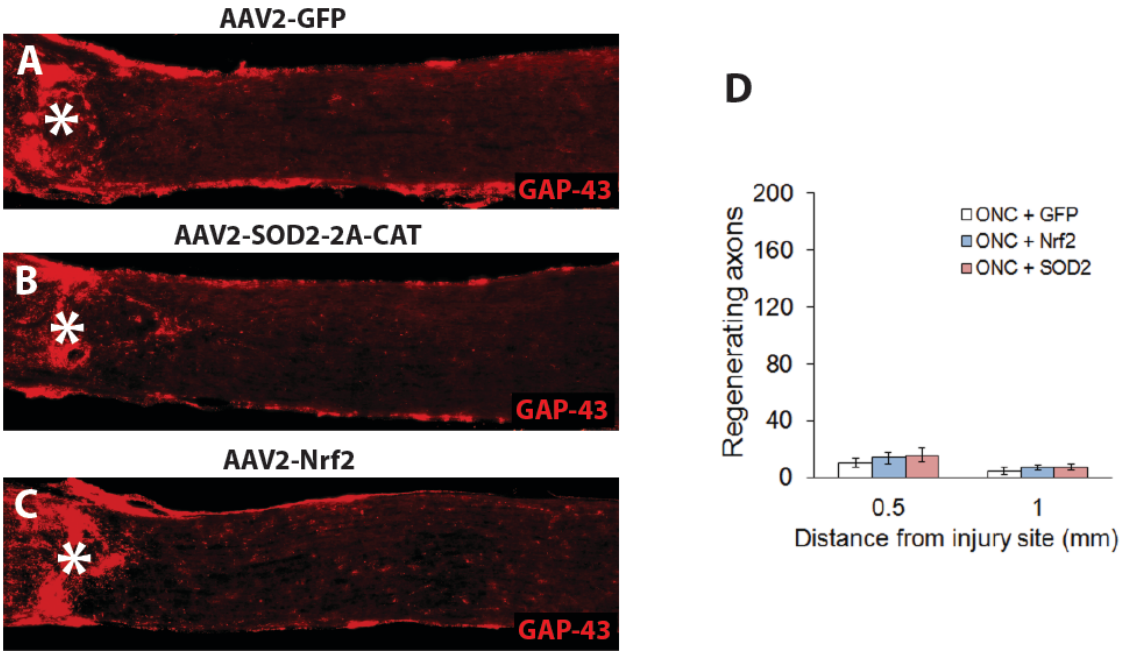

Figure S7. Axon regeneration was not promoted by overexpression of Nrf2. Longitudinal sections through the optic nerve showing GAP-43 positive axons 2 weeks after optic nerve crush (ONC). Overexpression of SOD2 plus catalase (B), overexpression of Nrf2 (C) by AAV2 vectors do not promote axon regeneration compared to the AAV2-GFP control treatment (A). D) Quantification of the number of axons that reach 0.5mm and 1.0mm from injury sites (marked by asterisk).

Table S1

age / treatment group (mouse genotype)	P30	P50	P70	P80
***untreated* (*CD1*)**	338±9 (n=3)	345±9 (n=4)	347±9 (n=3)	NA
AAV-GFP (*rd1*)	319±10 (n=8)	131±10 (n=29)	76±10 (n=29)	63±4 (n=3)
AAV-GFP+ AAV-SOD2-2A-CAT (*rd1*)	326±17 (n=7)	196±8 (n=7)	80±9 (n=48)	NA
AAV-GFP+ AAV-Nrf2 (*rd1*)	310±7 (n=3)	255±17 (n=8)	159±12 (n=5)	NA
AAV-GFP+ AAV-PGC1a (*rd1*)	174±17 (n=3)	106±9 (n=15)	NA	31±6 (n=3)
AAV-GFP+ AAV-Nrf2+ AAV-PGC1a (*rd1*)	313±5 (n=6)	241±9 (n=10)	NA	117±12 (n=3)

Table S1. Cone quantification data shown in Figure 4H. Numbers represent mean±s.e.m.. The number of retinas examined in each group was shown in the parentheses.